Application of Pareto Approach to Improve the State Dependent Ricatti Equation (SDRE) Controller Performance

Luiz C. G. De Souza, Pierre G. Bigot, Alain G. De Souza

Abstract–The main objective of this work is to study the State Dependent Riccati Equation (SDRE) regulator; an adaptive Linear Quadratic Regulator (LQR) which allows to deal with the non linearities of the system to be controlled. In order to use this controller, a nonlinear mathematical model of a flexible rotatory beam is built through the Lagrangian formulation which can represent a rigid-flexible satellite. The flexible displacement is modelled using the assumed modes theory and a structural damping is added applying the Rayleigh technique. There are two main objectives related to control: the first one is to control the hub angular position and the second one is the need to minimize flexible displacements of the satellite panel. Doing computational simulations, it is possible to draw the performance map of the system which map all SDRE reachable performances. Then, a sorting algorithm enables to get the Pareto's border which represents the set of optimal performances. On the other hand, analyzing the influence of the weight matrixes terms, it is shown that it is possible to get the Pareto's border performances using only a few terms of the SDRE weight matrixes. On the basis of this analysis, a law enabling to get weight matrixes' values in function of a required performance is developed. Last of all, state dependent weight matrixes are used to show that they can improve the system performance. Based on the results, it turned out that the SDRE's performance is better than the LQR's one, not only because it can deal with non linearities, but also because its design is more flexible.

Keywords–SDRE, dynamic of flexible beam, nonlinear control law

I. ITRODUCTION

THE main interest of the SDRE method [1] is that it is a systematic approach that can deal with non-linear plant. A good state of the art about SDRE theory can be found in [2]. The idea of SDRE is to linearize the plant around the instantaneous point of operation, producing a constant state space model and then calculate the controller as in LQR control technique [3].

This work was supported by the Conselho Nacional de Desenvolvimento Científico e Tecnológico, CNPq, Brasil, under Grant 400164/2016-7.

Luiz Carlos Gadelha de Souza. Federal University of ABC , Av. dos Estados, 5001 - Santo André - SP, 09210-580 Brasil. (phone: +55 (61) 99845-2804, e-mail: lcgadelha@ gmail.com).

Pierre Bigot National Institute for Space Research – Av. Dos Astronautas, 1758, Sao Jose dos Campos – SP, 12227-010 Brasil. (email: pierre.bogot.01@gmail.com).

Alain Giacobini de Souza. Instituto Tecnologico da Aeronautica. Praça Marechal Eduardo Gomes, 50 - Vila das Acacias, São José dos Campos - SP, 12228-900 Brasil (e-mail: alaingiacobini@gmail.com).

The process is repeated at each sampling periods producing and controlling several state dependent linear models out of a non-linear one. In other words, a SDRE controller is an adaptive LQR. Feasibility in real time could be a problem as the computation time for calculating the controller (solving the Algebraic Riccati Equation ARE) has to be inferior to the sampling time of the system. Therefore, several simulations have proven the computationally feasibility for real time implementation as in control of missiles [4] and helicopter [5]. A different approach, also based on na optimization of weight matrix was applied by [6], [7] and [8] to design a control system of flexible satellites. As feasibility has no more to be proven, therefore, this study will focus on simulation and will show benefit of a non-linear weighting.

II. SDRE METHODOLOGY

One of the most important contributions for SDRE control is the Linear Quadratic Regulation (LQR). LQR is an optimal controller minimizing a quadratic function cost given by

$$J_{\text{LQR}} = \frac{1}{2}\int_{t_0}^{\infty}(x^TQx + u^TRx)dt \tag{1}$$

where $x \in \mathbb{R}^n$ is the state vector, $u \in \mathbb{R}^m$ is the control signal, and, $Q \in \mathbb{R}^{n\times n}$ and $R \in \mathbb{R}^{m\times m}$ are the weight matrices semi defined positive and defined positive respectively.

The idea of this function is making a trade of between performances using the Q weight to regulate the "size" of the states x and energy saving using the R weight to regulate the control signal u. The SDRE approach is an extension of the LQR controller: it is based on the same quadratic cost function (1) with the difference that weights Q and R can be state dependent:

$$J_{\text{SDRE}} = \frac{1}{2}\int_{t_0}^{\infty}(x^TQ(x)x + u^TR(x)x)dt \tag{2}$$

To solve this optimization problem, it is needed to define the specific problem in order to get constraints of the cost function. There are two kinds of constraints: the model and initial conditions. It can be written as:

$$\dot{x} = f(x) + g(x)u, \qquad x(t_0) = x_0 \tag{3}$$

Applying a direct parameterization to transform the non-linear system of (3) into State Dependent Coefficients (SDC) representation (Souza, 2012), the dynamic equation of the system with control can be written in the form

$$\dot{x} = A(x)x + B(x)u \tag{4}$$

A is not unique. In fact there are an infinite number of parameterizations for SDC representation when the dynamic is non-linear. For the sake of example, let the dynamic function be a simple scalar function as

$$f(x_1,x_2) = 3x_1x_2 \quad (5)$$

Then A can take an infinite number of different forms as

$$\begin{aligned} A(x_1,x_2)\begin{bmatrix}x_1\\x_2\end{bmatrix} &= [3x_2 \quad 0]\begin{bmatrix}x_1\\x_2\end{bmatrix} \\ A(x_1,x_2)\begin{bmatrix}x_1\\x_2\end{bmatrix} &= [0 \quad 3x_1]\begin{bmatrix}x_1\\x_2\end{bmatrix} \\ A(x_1,x_2)\begin{bmatrix}x_1\\x_2\end{bmatrix} &= [2x_2 \quad x_1]\begin{bmatrix}x_1\\x_2\end{bmatrix} \end{aligned} \quad (6)$$

For multivariable case, it exists always at least two parameterizations A_1 and A_2 for all $0 \le \alpha \le 1$ satisfying

$$A(x) = \alpha A_1(x) + (1-\alpha)A_2(x) \quad (7)$$

Then $A(x,\alpha)$ represents the infinite family of SDC parameterization. The non-uniqueness of SDC parameterization creates additional degrees of freedom. The choice of parameterizations must be made in accordance with the control system of interest. However, this choice should not violate the controllability of the system, i.e., the state dependent controllability matrix must be full rank [8].

$$C_o(x) = [B(x) \quad A(x)B(x) \quad \dots \quad A(x)^{n-1}B(x)] \quad (8)$$

The State Dependent Algebraic Riccati Equation (SDARE) can be obtained applying the conditions for optimality of the variation calculus. In order to simplify expressions, state dependent matrix are sometimes written without reference to the states x: i.e. $A(x) \equiv A$. As a result, the Hamiltonian for the optimal control problem (2) and (4) is

$$H(x,u,\lambda) = \frac{1}{2}(x^TQx + u^TRu) + \lambda(Ax + Bu) \quad (9)$$

where $\lambda \in \mathbb{R}^n$ is the Lagrange multiplier.

Applying to (9) the necessary conditions for the optimal control given by $\dot{\lambda} = -\frac{\partial H}{\partial x}$, $\dot{x} = -\frac{\partial H}{\partial \lambda}$ and $0 = -\frac{\partial H}{\partial x}$ leads to

$$\begin{aligned} \dot{\lambda} = -Qx - \frac{1}{2}x^T\frac{\partial Q}{\partial x}x - \frac{1}{2}u^T\frac{\partial R}{\partial x}u \\ -\left[\frac{\partial Ax}{\partial x}\right]^T\lambda - \left[\frac{\partial Bu}{\partial x}\right]^T\lambda \end{aligned} \quad (10)$$

$$\dot{x} = A(x)x + B(x)u \quad (11)$$

$$0 = R(x)u + B^T(x)\lambda \quad (12)$$

Assuming the co-state in the form $\lambda(x) = P(x)x$, which is dependent of the state, and using (12), the feedback control law is obtained as

$$u(x) = -R^{-1}(x)B^T(x)P(x)x \quad (13)$$

Substituting this results into (11) gives

$$\dot{x} = A(x)x - B(x)R^{-1}(x)B^T(x)P(x)x \quad (14)$$

To find the function P, $\lambda = P(x)x$ is differentiated with respect to the time along the path

$$\dot{\lambda} = \dot{P}x + PAx - PBR^{-1}B^TP \quad (15)$$

Substituting (15) in the first necessary condition of optimal control (10) and arranging the terms more appropriately results in

$$\begin{aligned} 0 = \dot{P}x + \frac{1}{2}x^T\frac{\partial Q}{\partial x}x + \frac{1}{2}u^T\frac{\partial R}{\partial x}u \\ +x^T\left[\frac{\partial A}{\partial x}\right]^T Px + \left[\frac{\partial Bu}{\partial x}\right]^T Px \\ +(PA + A^TP - PBR^{-1}B^TP + Q)x \end{aligned} \quad (16)$$

Two important relations are obtained to satisfy the equality of (16). The first one is state-dependent algebraic Riccati equation (SDARE) which solution is $P(x)$ given by

$$PA + A^TP - PBR^{-1}B^TP + Q = 0 \quad (17)$$

Once $P(x)$ is known, it is possible to know our controller K explicitely. The expression of our controller can be extracted from (13)

$$K = R^{-1}(x)B^T(x)P(x) \quad (18)$$

The second one is the necessary condition of optimality which must be satisfied, it is given by

$$\begin{aligned} 0 = \dot{P}x + \frac{1}{2}x^T\frac{\partial Q}{\partial x}x + \frac{1}{2}u^T\frac{\partial R}{\partial x}u \\ +x^T\left[\frac{\partial A}{\partial x}\right]^T Px + \left[\frac{\partial Bu}{\partial x}\right]^T Px \end{aligned} \quad (19)$$

For some special cases, such as systems with little dependence on the state or with few state variables, (18) can be solved analytically. On the other hand, for more complex systems, the numerical solution can be obtained using an adequate sampling rate. An important factor of the SDRE method is that it does not cancel the benefits that result from the non-linearity of the dynamic system, because, it is not require inversion and no dynamic feedback linearization of the non-linear system.

III. EQUATIONS OF MOTION OF RIGID-FLEXIBLE SATELLITE

Figure 1 shows a representation of rigid-flexible satellite by a flexible rotatory beam; which consists of a beam fixed to the rotor motor at one end and free at the other one. Euler-Bernoulli beam is used; this means that deformations are considered small. Parameters of the beam are the following: length L, linear density ρ, rigidity EI_z and the rotor motor parameters are: angular position $\theta(t)$, which is a rotation along the X-axis so gravity has no influence, rotor and beam inertia J_{eq}, a characteristic constant of the motor C_m, the voltage U_m and radius of the hub r. The beam displacement is $y(x,t)$. To simplify notation, y is used without referring to its variables and its partial derivatives relative to the time t and the position x are respectively written $\dot{y}$ and y'.

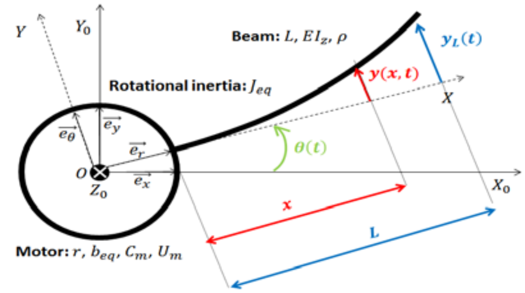

Fig.1 Representation of the rigid-flexible satellite model

The assumed mode method supposes that the flexible displacement is a linear combination of products of a space function $\Phi : x \rightarrow \Phi(x)$ (also called form) with a time function $q : t \rightarrow q(t)$ that we will call mode.

$$y(x,t) = \sum_{i=1}^{n} \Phi_i(x) q_i(t) = \Phi^T q = q \qquad (20)$$

Figure 2 represents a classical form function respecting physical boundaries for a clamped-free beam.

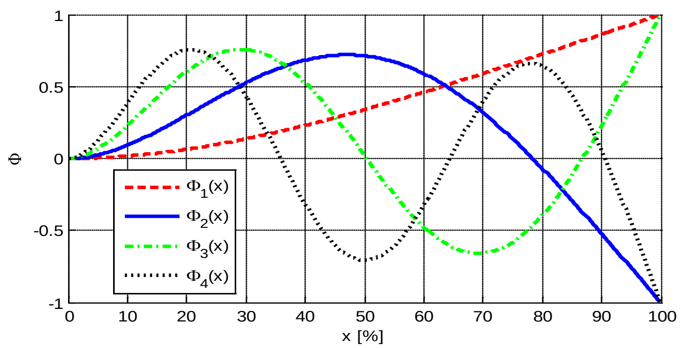

Fig. 2. First four form functions Φ(x)

Lagrange theory permits deriving non-linear motion equations. Full calculation can be found in [9].

$$M(q)\begin{bmatrix}\ddot{\theta}\\ \ddot{q}\end{bmatrix} + N(q,\dot{q},\dot{\theta})\begin{bmatrix}\dot{\theta}\\ \dot{q}\end{bmatrix} + K\begin{bmatrix}\theta\\ q\end{bmatrix} = FU_m \qquad (21)$$

It is a classical vibrating systems equation [11]: M the mass matrix, N the damping matrix, K the rigidity matrix and F the external force vector.

$$K = \begin{bmatrix}0 & 0\\ 0 & K_{ff}\end{bmatrix} \qquad F = \begin{bmatrix}C_m\\ 0\end{bmatrix} \qquad (22)$$

$$M = \begin{bmatrix}J_{eq} + q^T M_{ff} q & M_{rf}^T\\ M_{rf} & M_{ff}\end{bmatrix} Q_q$$
$$N = \begin{bmatrix}b_{eq} + q^T M_{ff}\dot{q} & q^T M_{ff}\dot{\theta}\\ -M_{ff} q\dot{\theta} & aM_{ff} + bK_{ff}\end{bmatrix} \qquad (23)$$

a and b are Rayleigh damping coefficients. It is a technic to model structural damping without having to know all materials properties [10]. Other matrix elements are defined in function of the form function as

$$M_{ff} = \int_0^L \Phi(x)\Phi^T(x)dx\,, M_{rf} = \rho\int_0^L (r+x)\Phi(x)dx\,, K_{ff} = EI_z\int_0^L \Phi''(x)\Phi''^T(x)dx \qquad (24)$$

It can be denoted in (23) and (24) represent the no linear equation of motion of the rigid-flexible satellite and where the mass M and damping matrix N are not constants and depends on $q, \dot{q}$ and $\dot{\theta}$.

To be able to apply the SDRE technique, this system has to be represented in the SDC form, with the system states x are the rigid mode θ and flexible modes q and their derivatives and control u are defined by

$$x = [\theta \quad q \quad \dot{\theta} \quad \dot{q}]^T \qquad u = U_m \qquad (25)$$

Reorganizing (21), the equations of motions of the rigid-flexible satellite in the classic state space representation given by

$$\dot{x} = \underbrace{\begin{bmatrix}0 & I\\ -M^{-1}K & -M^{-1}N\end{bmatrix}}_{A(x)} x + \underbrace{\begin{bmatrix}0\\ M^{-1}F\end{bmatrix}}_{B} u \qquad (26)$$

One observes that a and b are Rayleigh damping coefficients without considering its division into static and dynamics and that M and N are clearly states dependent as well as the matrices A and B are state dependent too.

IV. INTRODUCING THE DYNAMIC DAMPING

Considering that the damping of the system is different when the arm moves and when it is stopped, which means that it is difficult to start the rotation but, once the beam is in motion, the damping decreases. The damping can be considered in two ways: the static damping when $\dot{\theta} = 0$ and dynamic when $\dot{\theta} \neq 0$. Therefore, one represents the damping terms as a linear function of the angular velocity module by $\dot{\theta} = 0$

$$B_{eq} = B_{eq0} + k_{B_{eq}}|\dot{\theta}|$$
$$a = a_0 + k_a|\dot{\theta}| \qquad (27)$$
$$b = b_0 + k_b|\dot{\theta}|$$

This modeling for the Rayleigh coefficients is confirmed by [11] which states that the structural damping is generally non-linear and function of the displacement amplitude, once it is evident that when the angular velocity $\dot{\theta}$ increases the displacement as well. Considering the expressions of (27), the system Equation can be rewritten by

$$\underbrace{\begin{bmatrix} C_m \\ \mathbf{0_{n1}} \end{bmatrix}}_{F} \boldsymbol{U_m} = \underbrace{\begin{bmatrix} J_{eq} + \boldsymbol{q}^T \boldsymbol{M_{ff}} \boldsymbol{q} & \boldsymbol{M_{rf}^T} \\ \boldsymbol{M_{rf}} & \boldsymbol{M_{ff}} \end{bmatrix}}_{M} \begin{bmatrix} \ddot{\theta} \\ \ddot{\boldsymbol{q}} \end{bmatrix} + \underbrace{\begin{bmatrix} 0 & \mathbf{0_{1n}} \\ \mathbf{0_{n1}} & \boldsymbol{K_{ff}} \end{bmatrix}}_{K} \begin{bmatrix} \theta \\ \boldsymbol{q} \end{bmatrix}$$
$$+ \underbrace{\begin{bmatrix} B_{eq0} + k_{B_{eq}}|\dot{\theta}| + \boldsymbol{q}^T \boldsymbol{M_{ff}} \dot{\boldsymbol{q}} & \dot{\theta} \boldsymbol{q}^T \boldsymbol{M_{ff}} \\ -\boldsymbol{M_{ff}} \boldsymbol{q} \dot{\boldsymbol{\theta}} & (a_0 + k_a|\dot{\theta}|)\boldsymbol{M_{ff}} + (b_0 + k_l \end{bmatrix}}_{N}$$

It is noted in (28) that the damping matrix N has additional nonlinear terms. These terms can be joined in a matrix representing the dynamic damping $\boldsymbol{N}_{|\dot{\theta}|}$ such that N is now given by

$$\boldsymbol{N} = \underbrace{\begin{bmatrix} B_{eq} & \mathbf{0_{1n}} \\ \mathbf{0_{n1}} & \mathbf{0_{nn}} \end{bmatrix}}_{N_0} ++ \underbrace{\begin{bmatrix} \boldsymbol{q}^T \boldsymbol{M_{ff}} \dot{\boldsymbol{q}} & \boldsymbol{q}^T \boldsymbol{M_{ff}} \dot{\theta} \\ -\boldsymbol{M_{ff}} \boldsymbol{q} \dot{\theta} & \mathbf{0_{nn}} \end{bmatrix}}_{N_q} + \underbrace{\begin{bmatrix} 0 & \mathbf{0_{1n}} \\ \mathbf{0_{n1}} & a\boldsymbol{M_{ff}} + b\boldsymbol{K_{ff}} \end{bmatrix}}_{N_r} + \underbrace{\begin{bmatrix} k_{B_{eq0}}|\dot{\theta}| & \mathbf{0_{1n}} \\ \mathbf{0_{n1}} & k_a|\dot{\theta}|\boldsymbol{M_{ff}} + k_b|\dot{\theta}|\boldsymbol{K_{ff}} \end{bmatrix}}_{N_{|\dot{\theta}|}} \quad (29)$$

The proportionality coefficients of (27) for a, b e B_{eq} are given in Table I

TABLE I - STATIC AND DYNAMIC COEFFICIENTS OF VISCOUS AND STRUCTURAL DAMPING.

	Static coefficients $\dot{\theta} = 0$	Dynamic coefficients $\lvert\dot{\theta}\rvert = 0$
B_{eq}	0,1520	-0,046
a	-9,657	6
b	0,0207	-0,00067

Figure 3 shows the responses of this non-linear model comparing them with the expected responses of the real experiment.

In this simulation with dynamic damping, the result is much better, the response of the angular position is very good and is similar to that with the first set of parameters. In addition, the displacement of the beam tip is well represented, either during movement or at the end thereof, when the beam is stopped and vibrating.

It can be concluded that only a non-linear modeling of the system allows a good modeling of the actual experiment during all stages of the movement.

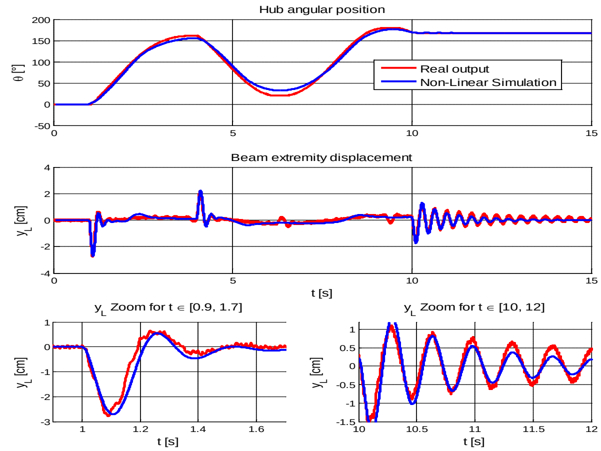

Fig. 3. Non-linear system response with the viscous and structural damping function of $|\dot{\boldsymbol{\theta}}|$

V. ANALISYS OF THE NO LINEAR TERNS INFLUENCE

An analysis of the nonlinear coefficient values of the terms M and N of (29) has been done by [12] permitted to know which of these terms are negligible. Basically, one compares the constant values and the variable values of the nonlinear terms of the model for a predefined motion. After this analysis (28) can be rewritten in more simplified form by

$$\underbrace{\begin{bmatrix} C_m \\ \mathbf{0_{n1}} \end{bmatrix}}_{F} \boldsymbol{U_m} = \underbrace{\begin{bmatrix} J_{eq} & \boldsymbol{M_{rf}^T} \\ \boldsymbol{M_{rf}} & \boldsymbol{M_{ff}} \end{bmatrix}}_{M} \begin{bmatrix} \ddot{\theta} \\ \ddot{\boldsymbol{q}} \end{bmatrix} + \underbrace{\begin{bmatrix} \mathbf{0} & \mathbf{0_{1n}} \\ \mathbf{0_{n1}} & \boldsymbol{K_{ff}} \end{bmatrix}}_{K} \begin{bmatrix} \theta \\ \boldsymbol{q} \end{bmatrix} + \underbrace{\begin{bmatrix} B_{eq0} + k_{B_{eq0}}|\dot{\theta}| & \dot{\theta} \boldsymbol{q}^T \boldsymbol{M_{ff}} \\ -\boldsymbol{M_{ff}} \boldsymbol{q} \dot{\boldsymbol{\theta}} & (a_0 + k_a|\dot{\theta}|)\boldsymbol{M_{ff}} + b_0 \boldsymbol{K_{ff}} \end{bmatrix}}_{N} \begin{bmatrix} \dot{\theta} \\ \dot{\boldsymbol{q}} \end{bmatrix} \quad (30)$$

From now on (30) will be the equation of motion of the rigid-flexible satellite used in the simulation.

VI. SDRE SIMULATION STRATEGY

As matrix A and B depends on the states their values must be determined on every step. So, for every iteration of the simulation, states vector x is measured, the Riccati solution P is obtained from (18) the feedback control u is determined thanks to (18) and then, the new matrix A is obtained. This process is described in the Fig.(4).

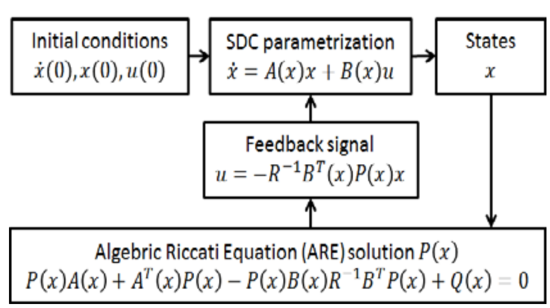

Fig. 4. SDRE algorithm

Implementation of this algorithm has been done using the MATLAB-Simulink. The solution of the Algebraic Riccati Equation (ARE) has been found via a S-function [13] which permits a faster computation of the solution in Simulink than calling the Matlab interpreter. The maximum voltage supply for the motor is ± 15V. Referring to performance objectives, those are temporal requirements since the model is non-linear and frequency analysis is not possible. The beam angular position θ has to stabilize in the region $\pm 5\%$ of the command θ_c in a minimum setting time: $T_{r5\%}$. Moreover, flexible deflection at beams extremity y_L has to be as smaller as possible and can't be higher than ± 1.5 [cm]. Note that this last condition is made in order to respect the small deformation hypothesis to get a valid model during all simulation.

Table 2 shows the values used for the simulation. It has been used 2 flexible modes. All results of simulation are obtained with the weight $R = 1$. The command signal used for all this study is $\theta_c = 90°$.

TABLE II - MODEL PARAMETERS VALUES

Beam	Values	Motor	Values
L	41.9 cm	b_{eq}	0.146 kg m^2 s^{-1}
EI_z	0.0913 N m	J_{eq}	0.00753 kg m^2
P	0.155 kg m^{-1}	C_m	0.1282 N V^{-1}

From the cost function represented by (2) it can be noted that weight Q is linked with the states x. Q weight is responsible for performance of the system. Q is a $(n+1) \times (n+1)$ matrix where n is the number of flexible modes. In order to influence each state independently Q has to be chosen a diagonal matrix, like : diag $\{Q_\theta, Q_q, Q_{\dot{\theta}}, Q_{\dot{q}}\}$. Increase Q results in faster regulation of the associated state [14]. This insight comes from the analysis of the function cost (2). Let x be a state of this system and Q_x its associated weight. Increasing the state x coeficient Q_x results in an increasing value of $x^T Q_x x$. To minimize this quantity, x has to reach the equilibrium value faster than other states. Weight terms can be seen as states penalties.

VII. INFLUENCE OF THE EACH TERMS OF MATRIX Q

First let's use the rigid-flexible satellite's equations of motion (26) to analyze the influence of each terms of Q independently. As it can be seen in Figure 5, increasing Q_θ leads to a faster system because θ state has to reach the equilibrium faster. Q_q and $Q_{\dot{q}}$ penalize flexible modes so one can see that the displacement is smaller when the weights increase. Finally $Q_{\dot{\theta}}$ penalize the angular speed, that's why the system takes a longer time to set up.

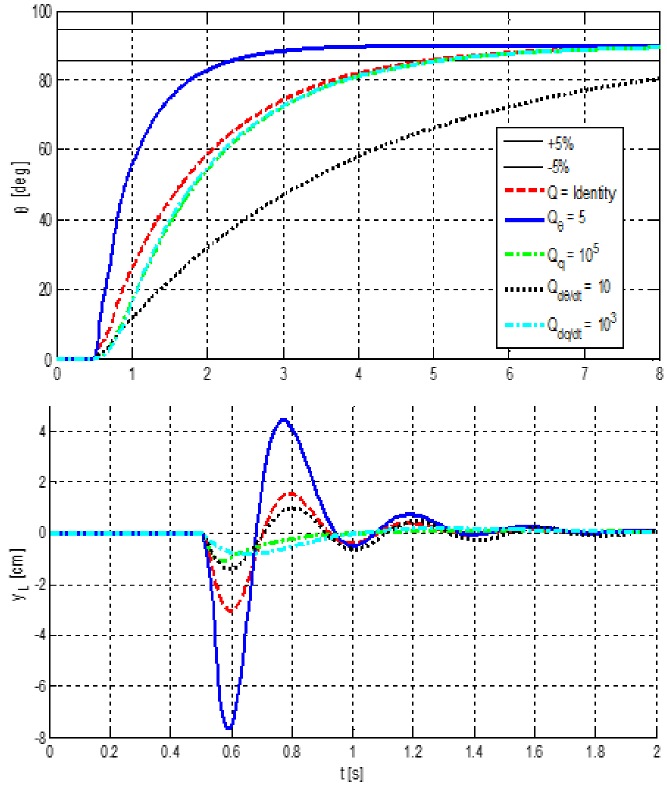

Fig. 5. Analyze of Q terms influence

To investigate the influence of flexible states one keeps the values of $Q_\theta = 10$ and $Q_{\dot{\theta}} = 1$ constants. Results have been represented in Figure 6. The best trade off found is the black response with $Q_q = 10^5$ and $Q_{\dot{q}} = 10^4$. The settling time is the same as the cyan response and the deflection is smaller. When looking at the green response and comparing to the black one, ones can see that the settling time is worse and the deflection gain in dropping the deflection is not so better. Note that values of Q_q and $Q_{\dot{q}}$ are high because values of q and $\dot{q}$ are small, remembering that what is to be minimized is $q^T Q_q q$ and $\dot{q}^T Q_{\dot{q}} \dot{q}$.

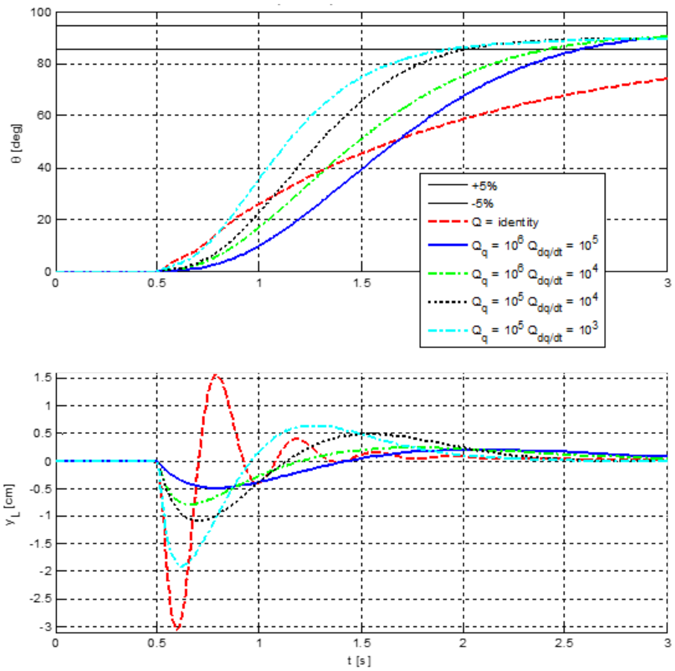

Fig. 6. Varying Q_q and Q_q˙ for Q_θ=10 and Q_θ˙ =1

The next step is to find good Q_θ and $Q_{\dot{\theta}}$. Other terms have been picked as the "best" value s of the previous analysis: $Q_q = 10^5$ and $Q_{\dot{q}} = 10^4$. As it is not an issue the way of getting the desired angular position (smoothly or not), $Q_{\dot{\theta}}$ can be relax. One relieves the constraint over $\dot{\theta}$, it means that there is no matter of $\dot{\theta}$ be high. Figure (7) shows that relaxing this constraint permits a better performance: green response is faster than blue response and displacement is almost the same. It has been verified that decrease $Q_{\dot{\theta}}$ more than 0.1 has no effective effect on the system.

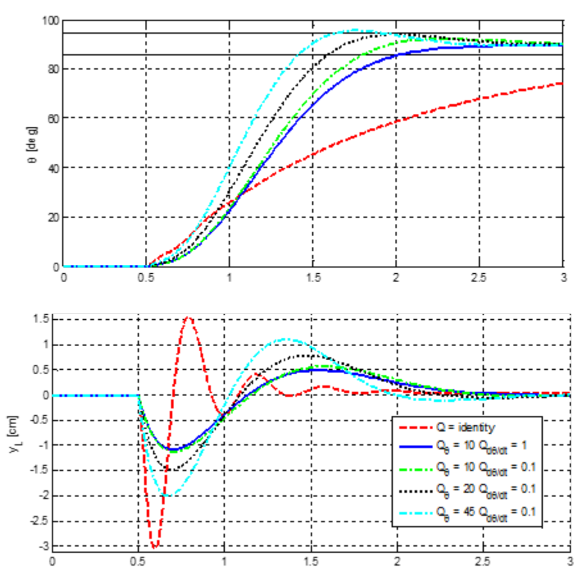

Fig. 7. Varying Q_θ and Q_θ˙ for Q_q=10^5 and Q_q˙ =10^4

On Figure 7 it is evident than increasing Q_θ improve the settling time but increase flexible deflections. Then designer has to choose in function of its most important requirement. For example if the settling time has to be inferior to 1 s, the cyan design is better; if the deflection can't be inferior to 1.5 cm, then the black design is more appropriate. From the results of Fig. 6 and 7, it can be see that flexible deflection is only important at the beginning of the motion. Then, to reduce this deflection, a small Q_θ is desired.

Therefore, to get a fast response, a high Q_θ is desired. The idea is to produce a variable Q_θ in function of the motion: small at the beginning of the motion and high at the end of the motion. The simpler function is a linear function of θ:

$$Q_\theta(\theta) = Q_{\theta_0} + \frac{K_{Q_\theta}|\theta - \theta_0|}{|\theta_c - \theta_0| + \epsilon} \tag{31}$$

Both Q_{θ_0} and K_{Q_θ} are scalar parameters of the linear function to adjust the law to get the desired performance. ϵ is a small number (typically 10^{-4}) to avoid singularity when $\theta_c = \theta_0$. When $t = 0$, $\theta(0) = \theta_0$ then, $Q_\theta(t_0) = Q_{\theta_0}$. At the contrary, when $t = t_\infty$, $\theta(\infty) = \theta_c$ then, $Q_\theta(\infty) \cong Q_{\theta_0} + K_{Q_\theta}$. So, it can be conclude that this function is increasing with the time, starting from Q_{θ_0} and getting to $Q_{\theta_0} + K_{Q_\theta}$.Note that this function is not a linear function of the time because $\theta(t)$ is not a linear function of time. To prove benefits of having such adaptive weight, the response for different weights $Q(\theta)$ has been calculated. The response is analyzed according two parameters: the setting time $T_{r5\%}$ and the maximum displacement at the beam extremity $y_{L_{max}}$. Figure 8 shows these two parameters for different combinations of $\{Q_{\theta_0}, K_{Q_\theta}\}$. Lines where Q_{θ_0} (colorful lines) and K_θ (black lines) are constant have been drawn. The resulting "performance map" is really helpful; it permits select weights $\{Q_{\theta_0}, K_{Q_\theta}\}$ easily to get a desired setting time or maximum deflection.

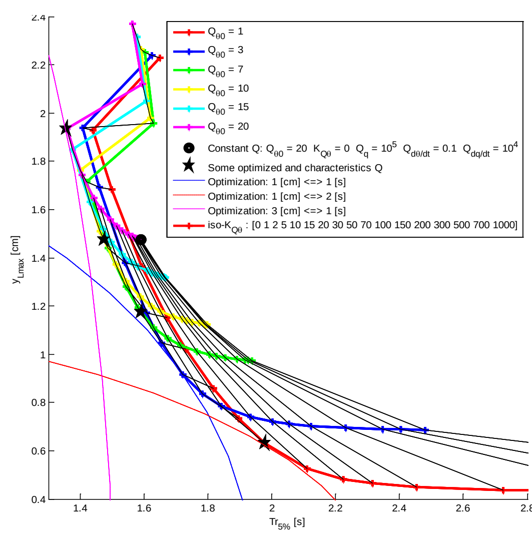

Fig. 8. Performance map {T_(r5%),y_(L_max) }

It also shows that a state dependent weight can improve performance: it exists faster response with the same maximum displacement and it exists a response with a smaller deflection having the same setting time. Constants Q_θ can be found at the right border of the map. For any of these constant weights a better state dependent weight can be found. Optimized combination of $\{Q_{\theta_0}, K_{Q_\theta}\}$ can be found on the left border of the map. For these points there is no other $\{Q_{\theta_0}, K_{Q_\theta}\}$ combination improving both $T_{r5\%}$ and $y_{L_{max}}$ performance parameter. In order to choose a combination of $\{Q_{\theta_0}, K_{Q_\theta}\}$ a simple optimization law can be adopted:

$$J_\theta = k_T T_{r5\%} + k_{y_L} y_{L_{max}} \quad (32)$$

If $k_T = k_{yL}$ it means that the importance of improving the setting time of 1[s] is the same as improving the deflection of 1[cm]. Graphically the best control minimizing 32 can be found as the intersection of the map and the smallest ellipse with origin in (0,0). In Figure 7 the ellipse for this first case is the blue dotted line. If time response if more relevant than deflection, the designer can augment k_T. For example if $k_T = 3k_L$ it would mean that improving the setting time of $1s$ is equivalent to improving the deflection of 3[cm]. This is the red dotted line in Figure 7. On the top of Figure 7, it seems there is a singularity: variation of $T_{r5\%}$ is not progressive: it jumps from a value to another. The explanation is simple, as $Q_{\theta 0}$ is higher, the system is faster. At some point the system is too much fast and it produces an overshoot of the response θ making $T_{r5\%}$ having a “step”.

Now, one shows the benefits of a state dependent weight comparing to a constant weight: the “best” constant Q: Q_0 previously found, which is $Q_0 = diag[20,\ 10^5, 0.1, 10^4]$. Responses for 4 different state dependent weights can be seen in Figure 9. The blue response is faster than with a constant Q with the same maximum deflection. The green response shows a smaller deflection with the same setting time. The black response is a “deflection optimized” response. Finally the cyan response is a “setting time optimized” response. Another advantage of this state dependent weight is that the flexible deflection is more “symetric”: there is not a huge diference between the first and second deflection. This behaviour can be helpful for system wich would rotate always the same way. If the deflection was not so symetric it could after intensive use appear a permanent deflection of the flexible beam due to the main flexible displacement always in the same direction.

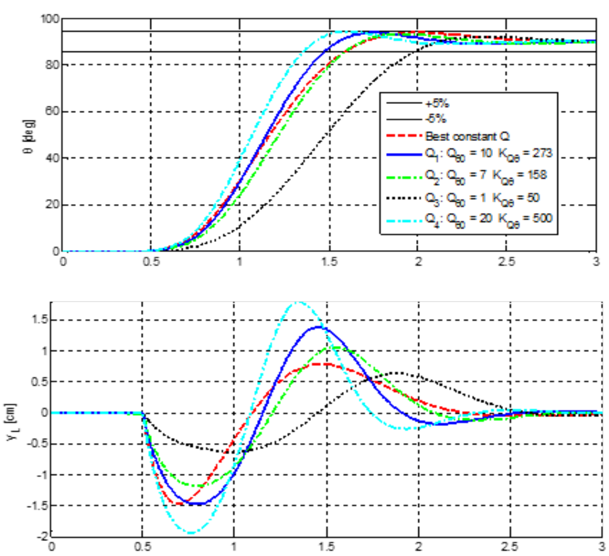

Fig. 9. Comparing states dependent Q_θ (θ) with the “best” constant one

VIII. MULTIOBJECTIVE OPTIMIZATION WITH PARETO APPROACH

In order to design an SDRE controller, it is necessary to choose values of the R and Q matrices. However, as seen all weights do not independently influence the performance objectives of the system makes it difficult to choose them. The goal is to find out what the values of the weight matrices that provides optimum performance to the system. Every difficulty of this problem comes from the fact that the performance of a system is not limited to a single parameter, but rather to a set of various performance parameters / objectives. These performance goals are often conflicting and a compromise between them is needed.

To make this choice in an analytical way, it is necessary to represent the performance objectives numerically [16]. For each objective, one defines a function $f_i: \boldsymbol{S} \rightarrow \mathbb{R}$, where S is the set of possible alternatives, in the SDRE controller, S is the set of possible weight matrices $\boldsymbol{S} = \{\boldsymbol{R}, \boldsymbol{Q}\}$. The set S is also called the design space or solution space.

In order to solve this multiobjective optimization problem, the different optimization objectives are aggregated into a single function that, being minimized, leads to a unique solution.

$$\text{Minimize}$$

$$F\ (x) = (f_1(x), f_2(x), \dots, f_k(x))\ for\ \ \boldsymbol{x} \in \boldsymbol{S} \quad (33)$$

The problem with this method is that the solution obtained depends heavily on the way in which the F function is constructed. A more practical approach to dealing with multiobjective problems is instead of finding a single solution heavily dependent on aggregations of optimization functions performed, find a set of optimal solutions; This set is knowledge as Pareto Frontier [16]. Applied in the context of multiobjective control theory, the Pareto frontier represents the set of optimal controllers: there is no other controller that can improve a system performance goal without harming at least one other performance goal.

The advantage of this approach is that it allows you to get a set of optimal controllers and then choose in a visual and graphical way which controller best matches your desired performance. When it has only two performance objectives, the performance space is reduced to two dimensions; in this case it is called a "performance map"

IX. CONTROL OBJETIVES, PERFORMANCE REQUIREMENTS AND MAP

The results of this section are obtained using the satellite 30. For the simulation only two modes of vibration are considered, i.e., n = 2. In this way, the system has six states, namely, $\boldsymbol{x} = [\theta \quad q_1 \quad q_2 \quad \dot{\theta} \quad \dot{q}_1 \quad \dot{q}_2]^T$. Consequently, the weight matrix Q is 6×6 in size. Also, since the system has only one control (the motor supply voltage $\boldsymbol{U_m}$), the vector of control signals is scalar: i.e. $\boldsymbol{u} = u = U_m$. Therefore, the weight matrix R is scalar, i.e., $\boldsymbol{R} = R$.

A. 6.1 Control objectives are

a) Minimize the time to stabilize the angle θ in a range ±5% of the desired angular value θ_c.

b) Minimize the maximum amplitude of the flexible displacementy_L.

c) Minimize the energy E_∞ required to perform the control of the movement.

These control objectives can be called performance parameters or goals. The notations adopted in this work for these three parameters $(T_{r5\%} \quad y_{Lmax} \quad E_u) \in (\mathbb{R}^+)^3$ are mathematically defined as

$$T_{r5\%} = min_{t\in[0,t_\infty]}(T \ \mid \theta(T+t) \in [0.95\theta_c \quad 1.05\theta_c]) \tag{34}$$

$$y_{Lmax} = max_{t\in[0,t_\infty]}|y_L(t)| \tag{35}$$

$$E_u = \int_0^{t_\infty} U_m^2(t)dt \tag{36}$$

B. Performance requirements are

a) The overshoot in the angular positioning should not exceed 5% of the desired value θc, thus, $\bar{\theta} = 5e^{-2}\,\theta_c$

b) It is established as maximum flexible displacement at the tip of 5 [cm], thus, $\overline{y_L} = 5e^{-2}$. This equation can be expressed as a function of the assumed modes $y_L = \mathbf{\Phi}^T(L)\boldsymbol{q}$, so choose $\bar{q}_i = \overline{y_L}/\Phi_i(L)$ where i∈ {1, 2}.

C. Control limitations are

a) The motor supply voltage is limited to ± 15 [V], therefore $\overline{U_m} = 15$..

b) It is considered that an angular velocity of the beam of one rotation per second is a high value, thus, $\bar{\dot{\theta}} = 2\pi$

c) It is considered that a flex speed of the beam tip of 5 [cm] and half a second is a high value, thus, $\overline{\dot{y_L}} = 0.1$. As $\dot{y_L} = \mathbf{\Phi}^T(L)\dot{\boldsymbol{q}}$, one choses $\bar{q}_i = \overline{y_L}/\Phi_i(L)$ where $i \in \{1,2\}$.

D. Performance map

The performance map is a graph having two axes representing the system performance goals. Each point in this map is obtained by simulating the system with a different SDRE controller configuration, that is, with different values of the weights of the Q and R matrices. Figure 10 represents the performance map for the objectives $T_{r5\%}$ and y_{Lmax} associated with various values of the matrices weights $R = R_u\,\bar{\bar{R}}$ and $\boldsymbol{Q} = \text{diag}(Q_\theta, Q_q\boldsymbol{I_2}, Q_{\dot{\theta}}, Q_{\dot{q}}\boldsymbol{I_2})\overline{\boldsymbol{Q}}$.

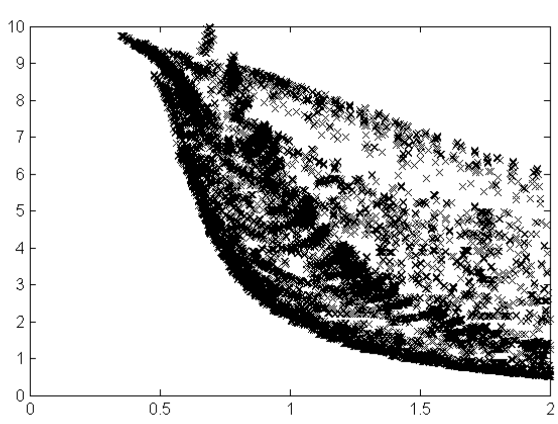

Fig. 10 - Performance map of the SDRE controlled obtained with several different control weights Q and R.

From Fig. 10, it can be seen the system performances map of SDRE controller. The division of these points is not uniform; some sets of points appear in the left Pareto border which represents the best attainable performances. In this area the density of points is very high; this means that there are many different combinations of weights that allow optimum performance. In between of the Pareto area also has a high dot density. These points represent the overshoot performances in the response θ. Typically, when attempting to increase the speed of the system, a time arrives where the value of θ to be reached (θ_c) is exceeded, this causes the stabilization time of the system $T_{r5\%}$ to increase abruptly, creating a zone of relatively low point density between the left and right sets of points.

X. CONPARISON OF THE LQR ND SDRE PERFORMANCE CONTRLLERS

The major advantage of the SDRE controller compared to the LQR controller is to be able to consider the nonlinearities of the model, soit is expected that the use of the SDRE-type controller will achieve better performance than the LQR controller. In the same way that the SDRE performance map was obtained, it is possible to obtain the peformance map of the LQR by a large combination of weights. This comparative study is presented in Figure 11. The Pareto boundaries of SDRE and LQR are represented in red and green respectively. It is noticed that the SDRE controller achieves better performances than the LQR controller because the red curve is below the green curve. The gain in performance is not very large, probably because the modeled system does not have very large nonlinearities. It is believed that this gain would be greater for a system with higher nonlinearities.

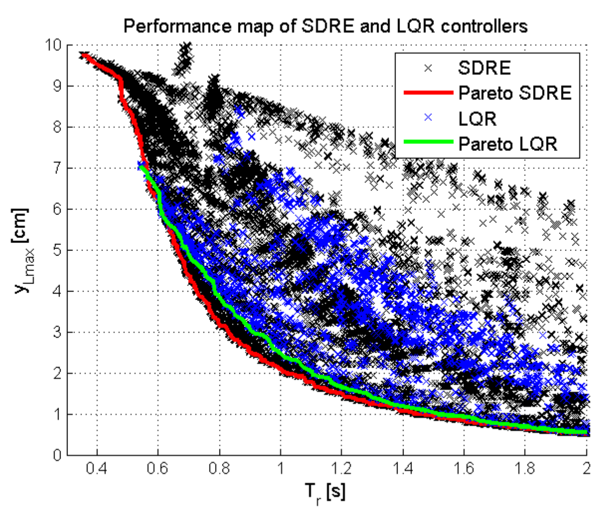

Fig. 11 Comparison of performance map and Pareto frontier of SDRE and LQR controllers.

Now a comparative study of the LQR and SDRE controller performance using constant weights for the first and the SDRE controller using state dependent weights. Two advantages of the SDRE controller has over the regular LQR: first, it allows considering the nonlinearities of the system to be controlled and second, it is possible to use weights that depend on the state of the system. These two advantages translate into a gain in considerable system performance.

Three points are identified in Fig.10, each one being on the Pareto border of a performance map and respecting the condition y_Lmax < 3 [cm]. Looking at these three points, there is a gain in the stabilization time of approximately 0.1s between the LQR and the SDRE and between the SDRE and the state-dependent SDRE. In total the time of 0.2s between LQR and SDRE using state dependent weights.

Figure 12 shows the time domain responses of the three points identified in Figure 11. In addition to improving the stabilization time of the system having a maximum flexible displacement equal Lmax = 3cm, the SDRE consumes less energy to perform the maneuver. In addition, it is noted that when using SDRE with a state-dependent weight matrix, the second peak of the flexible displacement is larger and reaches almost the same level as the first (3cm). This phenomenon can be considered as positive because it allows the deformation of the beam during the maneuvers to be symmetrical on both sides and thus decreases the possibility of the beam presenting a residual deformation (due to material hysteresis) in one direction when the maneuver is performed.

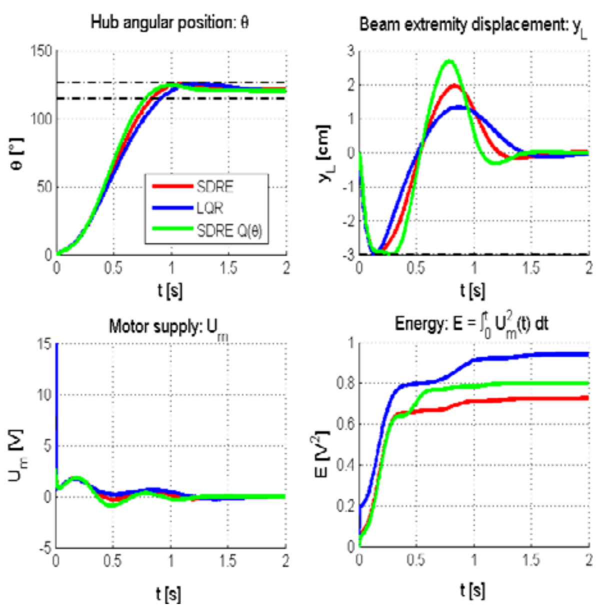

Fig. 12 - Comparison of best performance with $Y_{\_Lmax}$ <3 [cm] for the LQR and SDRE controllers using constant weights and SDRE using the weight Q (θ) dependent on the state θ.

XI. CONCLUSIONS

In this paper the SDRE controller was studied applying it to a non-linear model of a rigid-flexible rotating robotic arm formed by a flexible rod coupled to a servomotor. The elaborated model considers an Euler-Bernoulli type beam, uses the assumed modes method with two modes of vibration, considers first order nonlinearities and has a Rayleigh type structural damping. This model can be adapted to allow the simulation of satellites with flexible appendices such as antennas or solar panels. The mathematical model was validated by comparing the open-loop results with the real system results. The dynamics equations were parameterized to arrive at the SDC form for the implementation of the SDRE controller. The adjustment of the SDRE controller by means of the Q and R matrices was studied in detail: a normalization technique was applied in order to be able to perform simulations to measure the influence of each term of the matrices weight on the performance of the system. Afterwards, we tried to obtain the best possible performance in terms of system stabilization time and vibration minimization. For this, the performance map of the SDRE-controlled system was created to find the Pareto frontier; Set of optimal performance points. Based on the points of the Pareto frontier, a law was successfully created that allows to obtain the values of the matrices weight as a function of the value of a parameter of performance. The developed law has a limitation; It only works for a certain range of performance. Finally, a weight-dependent matrix of a state was used to show that, in this way, the performance of the SDRE can be improved. The study was concluded showing that the SDRE controller allows obtaining a better performance than the regulator LQR.

ACKNOWLEDGMENT

The authors would like to thank CAPES and INPE/DMC.

REFERENCES

[1] Cloutier J. R., DSouza C. N. and Mracek C. P. (1996). Nonlinear Regulation and Nonlinear H-infinity Control via the State-Dependent Riccati Equation Technique: Part 1. Theory. In Proc. of the 1st International onference on Nonlinear Problems in Aviation and Aerospace.

[2] Cimen, T. (2008, July). State-dependent Riccati equation (SDRE) control: a survey. In Proc. of the 17th IFAC world congress (pp. 3761-3775).

[3] Souza, L. C. G. (2006). Design of Satellite Control System Using Optimal Nonlinear Theory. Mechanics based design of structures and machines, 34(4), 351-364.

[4] Menon, P. K., Lam, T., Crawford, L. S., and Cheng, V. H. L. (2002). Real-time computational methods for SDRE nonlinear control of missiles. In American Control Conference, 2002. Proceedings of the 2002 (Vol. 1, pp. 232-237). IEEE.

[5] Bogdanov, A. and Wan, E. A. (2007). State-dependent Riccati equation control for small autonomous helicopters. Journal of guidance, control, and dynamics,30(1), 47-60.

[6] Sales, T.P.; Rade, D. A. and Souza, L.C.G. . Passive vibration control of flexible spacecraft using shunted piezoelectric transducers. Aerospace Science and Technology (Imprim), v. 1, p. 12-26, 2013.

[7] Souza, A. and Souza, L., ”H Infinity Attitude Controller Design for a Rigid-Flexible Satellite Considering the Parametric Uncertainty,” SAE Technical Paper 2016-36-0377, 2016, https://doi.org/10.4271/2016-36-0377.

[8] Pinheiro, E. R.; Souza, L. C. G.. Design of the Microsatellite Attitude Control System Using the Mixed Method via LMI Optimization. Mathematical Problems in Engineering (Print), v. 2013, p. 1-8, 2013.

[9] Souza, L. C. G. ans Gonzales, R. G. (2012). Application of the state dependent Riccati equation and Kalman filter techniques to the design of a satellite control system. Shock and vibration, 19(5), 939-946.

[10] Hammett, K. D., Hall, C. D. and Ridgely, D. B. (1998). Controllability issues in nonlinear state-dependent Riccati

equation control. Journal of guidance, control, and dynamics, 21(5), 767-773.

[11] Souza, A.G, Souza, L. C. G, H infinity controller design to a rigidflexible satellite with two vibration modes, Journal of Physics: Conference Series, vol. 641, pp. 012030, 2015.

[12] Bigot, P. and Souza, L. C. (2014). Investigation of the State Dependent Riccati Equation (SDRE) adaptive control advantages for controlling non-linear systems as a flexible rotatory beam. International journal of systems applications, engineering and development. (Vol. 8, pp 92-99)

[13] Wilson E. L. (1998). Three-Dimensional Static and Dynamic Analysis of Structures, Chapter 19. www.edwilson.org/BOOK-Wilson/19-DAMP.pdf

[14] WILSON, E. Linear Viscous Damping. In: Three Dimensional Static and Dynamic Analysis Of Structures. Berkeley, California: Computers and Structures, 1996.

[15] POLITYKO, E. Calculation of Pareto points. Matlab Central File Exchange,,2008. Disponvel em: ¡http://www.mathworks.com/matlabcentral/fileexchange/22507-calculation-of-pareto-points#comments¿

[16] Campa G., (2001). Algebric Riccati Equation solution in Simulink via C+fortran. Matlab Central File Exchange.

[17] Mracek, C. P. and Cloutier, J. R. (1998). Control designs for the nonlinear benchmark problem via the statedependent Riccati equation method. International Journal of robust and nonlinear control, 8(45), 401-433.

[18] SAWARAGI, Y.; NAKAYAM, H.; TANINO, T. Theory of multiobjective optimization. Orlando, Florida: Harcourt, 1985.